THE JOURNAL OF PHYSICAL CHEMISTRY C

Article

pubs.acs.org/JPCC

Molecular Resolution of the Water Interface at an Alkali Halide with Terraces and Steps

Fumiaki Ito,[†] Kei Kobayashi,[*,†,‡] Peter Spijker,[§] Lidija Zivanovic,[§] Kenichi Umeda,[†] Tarmo Nurmi,[∥] Nico Holmberg,[∥] Kari Laasonen,[∥] Adam S. Foster,[*,§,⊥] and Hirofumi Yamada[†]

[†]Department of Electronic Science and Engineering, Kyoto University, Kyoto 615-8510, Japan

[‡]The Hakubi Center for Advanced Research, Kyoto University, Kyoto 615-8520, Japan

[§]COMP Centre of Excellence, Department of Applied Physics, Aalto University, Helsinki FI-00076, Finland

[∥]Department of Chemistry, Aalto University, Helsinki FI-00076, Finland

[⊥]Division of Electrical Engineering and Computer Science, Kanazawa University, Kanazawa 920-1192, Japan

Supporting Information

ABSTRACT: Hydration structures at crystal surfaces play important roles in crystal growth or dissolution processes in liquid environments. Recently developed two-dimensional (2D) and three-dimensional (3D) force mapping techniques using frequency-modulation atomic force microscopy (FM-AFM) allow us to visualize the hydration structures at the solid−liquid interfaces at angstrom-scale resolution in real space. Up to now, the experimental and theoretical studies on local hydration structures have mainly focused on those on the terrace, but little work has looked at step edges, usually the key areas in dissolution and growth. In this study, we measured local hydration structures on water-soluble alkali halide crystal surfaces by 2D force mapping FM-AFM. The atomic-scale hydration structures observed on the terraces agree well with molecular-dynamics (MD) simulations. We also measured the hydration structures at the step edge of the NaCl(001) surface, which was constantly dissolving and growing, leading to the clear observation of atomic fluctuations. We found, with the support of MD simulations, that the hydration structures measured by FM-AFM at a time scale of a minute can be interpreted as the time-average of the hydration structures on the upper terrace and those on the lower terrace.

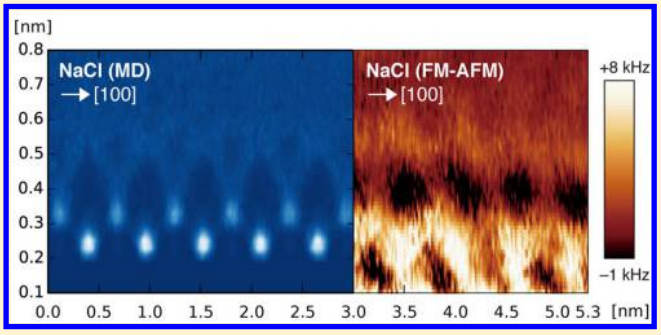

INTRODUCTION

Water molecules often form structured hydration layers at the solid−liquid interface, with characteristic oscillatory density profiles as a function of the distance from the surface.[1] The hydration structures are strongly related to various physical and chemical phenomena including crystal growth and dissolution processes. For example, hydration structures at the crystal step edges play key roles in processes such as solute adsorption and desorption at step edges.[2] The hydration structures have been experimentally measured by X-ray reflectivity;[1] however, it has been difficult to study atomic-scale hydration structures at the step edges. Recently, two-dimensional (2D) and three-dimensional (3D) force mapping techniques using frequency-modulation atomic force microscopy (FM-AFM) have been developed, now allowing us to visualize the hydration structures at the solid−liquid interfaces at angstrom-scale resolution in real space.[3−9] Up till now, many studies have been focused on the hydration structures on materials that are insoluble or difficult to dissolve in water in order to increase stability during the measurements.

In this study, we investigated the local hydration structures of water-soluble alkali halide crystals in their saturated aqueous solutions using the FM-AFM 2D force mapping technique. We studied the hydration structures on the (001) surfaces of KBr and NaCl crystals, both of which have a very high solubility in water, 5.5 and 6.1 mol/L (both at 20 °C), respectively.[10] Alkali halide crystals are relatively simple and the hydration structures of water on these crystals, especially those on the NaCl(001) surface, have been theoretically studied extensively,[11−14] but without the context of FM-AFM measurements providing molecular resolution. In this paper, we first discuss the hydration structures on the NaCl(001) and KBr(001) terraces based on the 2D force mapping FM-AFM experiments and the molecular dynamics (MD) simulations. Then, we also discuss the origin of the contrast in the 2D frequency shift map measured at a step edge on the NaCl(001) surface.

METHODS

Experimental Section. KBr and NaCl crystals purchased from Furuuchi Chemical were glued on a stainless plate and

Received: June 5, 2016
Revised: August 3, 2016
Published: August 10, 2016

DOI: 10.1021/acs.jpcc.6b05651
J. Phys. Chem. C 2016, 120, 19714−19722

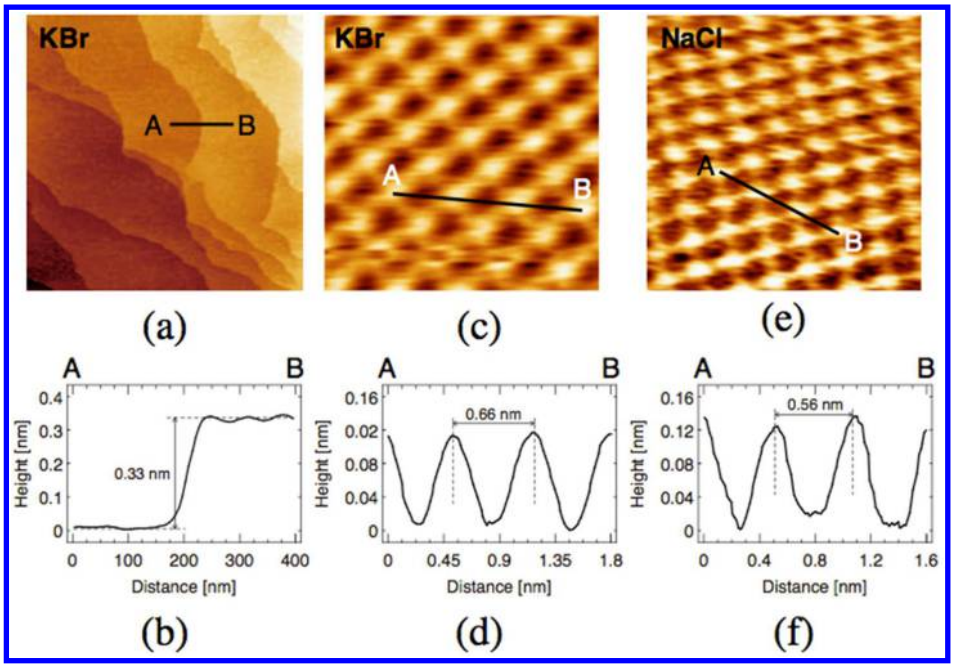

Figure 1. (a) Topographic image of the KBr(001) surface with a large scan area. Scanned area was 1.5 μm × 1.5 μm. (b) Cross-sectional height profile measured along the line A−B indicated in (a). (c) Atomic-scale topographic image of the KBr(001) surface. Scanned area was 2.6 nm × 2.6 nm (A_{p-p} = 0.8 nm, Δf = +450 Hz). (d) Cross-sectional height profile measured along the line A−B indicated in (c). (e) Atomic-scale topographic image of the NaCl(001) surface. Scanned area was 3.2 nm × 3.2 nm. (A_{p-p} = 0.8 nm, Δf = +450 Hz). (f) Cross-sectional height profile measured along the line A−B indicated in (e).

cleaved with a blade. The solution was kept nearly saturated such that the growth or dissolution rate of the crystal was lowered.[15] We used an FM-AFM instrument working in liquids that we developed based on a commercial AFM (SPM-9600, Shimadzu) with home-built electronics and a home-built controller using a field-programmable gate array module programmed with LabVIEW (National Instruments).[6] The resonance frequency was detected either by a home-built[16] or a commercially available phase-locked loop (PLL) circuits (HF2PLL, Zurich Instruments). We used Si cantilevers with a backside Au coating (PPP-NCHAuD, Nanosensors) and a nominal spring constant of 40 N/m. The cantilever was immersed in the solution, and the resonance frequency in the solution was about 130 kHz. We used an intensity-modulated blue-violet laser to excite the cantilever oscillation (photothermal excitation method).[17] The AFM instrument was placed in a temperature-regulated enclosure (CN-40A, Mitsubishi Electric Engineering), in which the temperature was kept at 20 ± 0.1 °C.

The procedure to obtain a 2D frequency shift map is as follows.[6] The tip was approached to the sample surface, and the tip−sample distance was controlled by keeping the frequency shift constant. After the tip−sample distance feedback control was disabled, a 2D frequency map (z−x slice) was collected in the z−x plane. At each x position, the frequency shift versus distance curve was recorded while the tip was approached to the sample surface by applying a triangular waveform signal of 10 Hz. The signal was immediately stopped when the frequency shift signal reached a predetermined threshold value (Δf_{th}), and the tip was retracted to the original position. The frequency shift curve was converted to the force curve using the analytical equation by Sader and Jarvis.[28]

Theoretical. On the basis of the face-centered cubic lattice structure of the alkali halide crystals, we built KBr and NaCl crystals measuring eight unit cells in each of the three dimensions, ensuring the (001) face is exposed. Each crystal thus consists of 4096 atoms, but the actual size depends on the lattice constant of the respective alkali halide (6.6 Å for KBr and 5.6 Å for NaCl). The crystals are first allowed to relax before water is added on either side of the exposed (001) plane, ensuring a water thickness of at least 4 nm on top of the crystal. The obtained solvated system (with approximately 7000 water molecules) is charge neutral and periodic in all three dimensions. In the case of systems with step edges, half the atoms on one of the exposed (001) planes have been removed, creating a rectangular pit with the step edge running along the [010] direction.

To describe all the interactions the CHARMM force field has been used.[19] All simulations have been performed using the MD code NAMD.[20] For visual inspection, VMD[21] was used and most of the analysis was performed using the Python library MDAnalysis.[22] For each of the MD simulations, a protocol is followed, similar to the setup used previously to study the interaction between calcite, water, and ions[23] and muscovite mica, water, and ions.[24] This includes an initial minimization of the energy associated with the water only (allowing bad contacts to be removed), followed by a short dynamics run of 10 ps to equilibrate the entire system at ambient conditions, and finally the production run of 250 ps. As the systems are typically very well behaved, we observe the typical hydration structure to be formed already after the equilibration phase. The relative short production run is sufficient to gather enough statistics for all our required analysis. For the systems with step edges, we employ an additional constraint on all the crystal atoms, preventing the crystal from dissolving: all atoms are constrained to their initial positions by a weak harmonic spring (k = 1.0 kcal/mol). Even though the process of dissolution is of great interest, empirical

DOI: 10.1021/acs.jpcc.6b05651
J. Phys. Chem. C 2016, 120, 19714−19722

force fields like CHARMM are not designed to capture all the dynamics correctly. Preventing the dissolution to happen ensures that we can focus on the hydration structure around the step edges instead. In all simulations the temperature and pressure are maintained to resemble ambient conditions.

Though a conversion method of the frequency shift to the interaction force is established,[18] it is not easy to predict the interaction force between the tip and the water molecules from the water density without performing extensive and computationally intensive free energy calculations of the system incorporating the tip.[25,26] However, as a first approximation, a recently proposed solvent tip approximation (STA) model can quickly provide a possible interaction force distribution.[27−29] In this study, we employed the STA model to compute the interaction force from the water density profile. The method is based on the assumption that the interaction force detected by FM-AFM is the variation in the free energy of the system caused by the displacement of a single water molecule at the tip apex. In the force versus distance curve in the approaching direction by the STA model, the attractive force corresponds to the onset of the hydration layer (decrease in the free energy) and the repulsive force corresponds to the tail of the hydration layer (increase in the free energy). The STA model has been successfully used to reproduce the interaction force profiles calculated by the free energy calculation of the system including the cluster tip model[27] as well as those observed experimentally on fluorite-water interfaces by FM-AFM.[29]

RESULTS AND DISCUSSION

Terrace. Figure 1a is a topographic image of the KBr(001) surface showing typical step and terrace structures. Despite that the scan rate was as slow as 0.24 Hz/line, the step edge was very sharp as shown in the cross-sectional height profile in Figure 1b. This is most likely because the image was taken 1 h after the immersion of the crystal into the saturated solution and the growth or dissolution processes were well suppressed. The profile shows that the step height was about 0.33 nm, which is in good agreement with the monatomic step height, a half of the lattice constant of KBr (0.66 nm). Although the edges appear to be sharp in Figure 1a, the profile showed that the step was not so sharp and the edge has a finite width of about 20 nm or more, because the step was fluctuating as discussed later. On the terrace of the alkali halide crystals, we often obtained atomic-resolution images (noting that this may reflect the atomic periodicity within the hydration structures[25]). Figure 1c,e are examples of those atomic-resolution images, which were taken on the KBr(001) and NaCl(001) surfaces, respectively, shown after the drift correction by comparing the two consecutively taken images with opposite slow scan directions. Figure 1d,f shows the cross-sectional height profiles measured on the A−B line on Figure 1c,e, respectively. The lines A−B were chosen such that they follow the brightest and darkest spots. Because the distance between the nearest neighbor bright spots was about 0.66 nm for KBr(001) and 0.56 nm for NaCl(001), the A−B lines run on the atomic rows along the [001] directions. From the cross-sectional profiles, we conclude that only one atomic position was observed as the bright spot in these atomic-resolution images.

We performed the 2D frequency shift mapping on both the KBr(001) and NaCl(001) surfaces. Figure 2a shows a 2D frequency shift (Δf) map measured on the KBr(001) surface in a plane perpendicular to the (001) surface. The slow scan direction (x) was on the atomic rows along the [001]

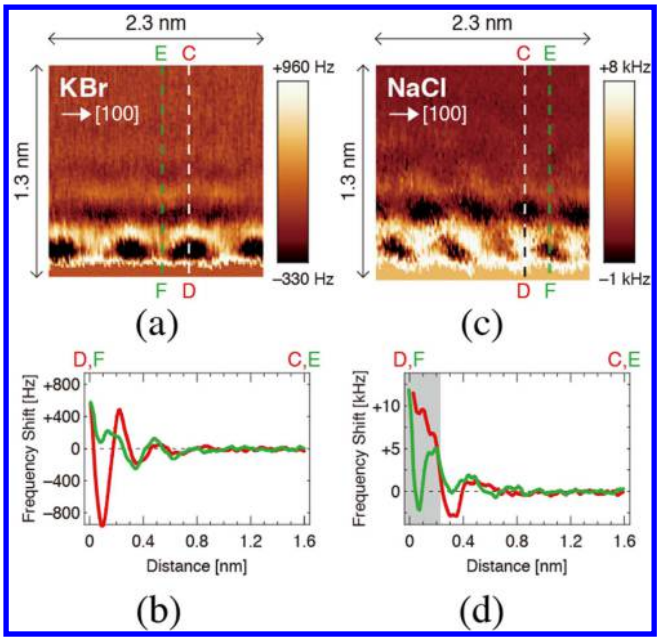

Figure 2. (a) 2D frequency shift map of a plane perpendicular to the KBr(001) surface along the [100] direction (A_{p-p} = 0.25 nm, Δf_{th} = 1 kHz). (b) Frequency shift versus distance curves along the lines C−D and E−F indicated in (a). (c) 2D frequency shift map of a plane perpendicular to the NaCl (001) surface along the [001] direction (A_{p-p} = 0.25 nm, Δf_{th} = 12 kHz). (d) Frequency shift versus distance curves along the lines C−D and E−F indicated in (c). The shaded region represents the region in which the data could not have been measured if the threshold frequency were set at 2 kHz.

directions. The 2D frequency shift map consists of the 256 frequency shift versus distance curves, which were recorded for about 30 s. The bright and dark contrasts correspond to the area with the positive and negative frequency shift, respectively. The featureless region at the bottom of the figures is the area without recorded data because the frequency shift reached the threshold value (Δf_{th}), which was about 1 kHz for Figure 2a. Therefore, the interface of the areas with and without the data corresponds to the cross-sectional topographic profile of the surface. We typically set Δf_{th} at about 1 kHz or a few kHz using the same cantilever with the same oscillation amplitude. If we set Δf_{th} to a larger value, we often observed a tip change that prevented us to stably obtain the 2D frequency shift map.

In Figure 2a, we found the characteristic dark blob features just above the interface with a lateral spacing of about 0.66 nm. We extracted the frequency shift curve along the line C−D in Figure 2a, as plotted in Figure 2b (red curve). The curve exhibited an oscillatory behavior and a large dip at the distance of about 0.1 nm. The origin of the distance was arbitrarily set. The characteristic period of the oscillation was about 0.3 nm, which is consistent with the size of the water molecule. We also extracted the frequency shift curve along the line E−F, which runs in between the dark blobs, as plotted in Figure 2b (green curve). The origins of the two curves were the same, that is, we did not shift the two curves with each other along the [001] direction. The two curves were roughly overlapping with each other in the distance range of about 0.4 nm and greater. However, the green curve along the line E−F did not show a large dip similar to the red curve, but rather showed a monotonic increase.

We also performed a 2D frequency shift map on the NaCl(001) surface. We routinely obtained the maps very

DOI: 10.1021/acs.jpcc.6b05651
J. Phys. Chem. C 2016, 120, 19714−19722

similar to those obtained on the KBr(001) surface as long as we set Δf_{th} at a small value, and they showed the characteristic dark blob features but did not show any remarkable differences from those taken on the KBr(001) surface except for the lateral periodicity (see Figure S1 in the Supporting Information). However, we once stably obtained a 2D frequency shift map even with the Δf_{th} raised to about 12 kHz, as presented in Figure 2c. Here, we also found the dark blob features with a lateral spacing of about 0.56 nm. Figure 2d shows the frequency shift curves along the lines C−D and E−F in Figure 2a. The shaded region in the figure represents the region in which the data could not have been measured if the threshold frequency were set at 2 kHz for illustrating the dependence of the threshold frequency on the measurement. In the frequency shift curve along the line C−D (red curve), we also observed a large dip at the distance of about 0.3 nm. The magnitude of the frequency shift minimum was greater than that in the case of the KBr(001) surface probably because of a different tip geometry. Although the origin of the distance was again arbitrarily set, we conclude that the tip was stable even though it moved about 0.2 nm closer to the surface, because the dip was at 0.1 nm from the surface in Figure 2a. On the other hand, we observed an oscillatory behavior in the green curve along the line E−F, which runs between the dark blobs. The curve also showed a dip at the distance of 0.1 nm. The characteristic period of the oscillation was again about 0.3 nm, which is consistent with the size of the water molecule. As the ionic radii of the hydrated ions in the solution are greater than the size of the water molecule, the observed contrasts on both the KBr(001) and NaCl(001) surfaces does not reflect the solvation structures of the hydrated ions, but the hydration structures. The density of the ions in the saturated solutions is about 6 mol/L, which is about one tenth of the water density in the bulk water (55.6 mol/L). Despite such a high ion concentration, we did not directly observe contrasts that can be attributed to the solvation structures of the hydrated ions nor adsorbed ions on the surface. However, a high concentration of ions in the solution plays a role in enhancing the image contrast of the hydration layers,[3−9,25] which could be partly that the structured water layers are more stable with the presence of the solute ions and the stable hydration structures can be more easily detected by AFM. Previous MD simulations[24,30,31] have shown that the residence time of the water molecules, as well that of the solute ions at the interface, is increased compared to that in the bulk solution, which could make the hydration structures more stable. This is because the effective concentration of the solute ions is higher at the interface than its bulk value.[30]

Figure 3a shows the water density distribution obtained from the MD simulations in a plane along the [001] direction on the KBr(001) surface. Figure 3b shows the density profile as a function of the distance from the surface on K^+ (red) and Br^- (green) ions (an average over every cation or anion position). Figure 3c,d shows the same data for NaCl. The contrasts have a periodic pattern along the [100] directions with a spacing of 0.66 and 0.56 nm for KBr and NaCl, respectively. The origin of the axis along the [001] direction is defined at the centers of the topmost atoms. The red and green blobs in the figures represent the ionic radii of the K^+, Br^-, Na^+, and Cl^- ions, which are modeled as the circle with a diameter of 0.13, 0.2, 0.1, and 0.18 nm, respectively. In Figure 3a,b, we can find the bright features above the cations and anions. They correspond to the regions at which the water density is much higher than the bulk

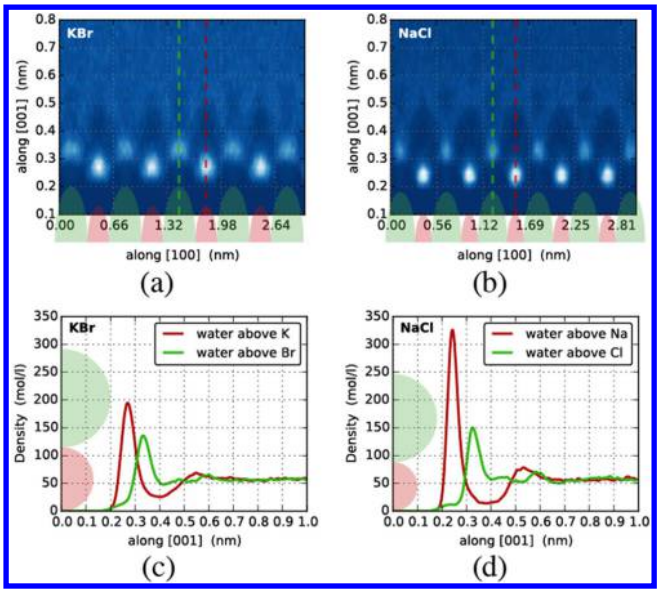

Figure 3. (a) 2D water density distribution in a plane along the [100] direction on the KBr(001) surface. (b) 2D water density distribution in a plane along the [100] direction on the NaCl(001) surface. (c) 1D water density profile on K^+ (red) and Br^- (green) ion as a function from the surface. Each curve presents the density of the water molecules on the half unit cell area (0.33 nm × 0.33 nm). (d) 1D water density profile on Na^+ (red) and Cl^- (green) ion as a function from the surface. Each curve presents the density of the water molecules on the half unit cell area (0.28 nm × 0.28 nm).

density; we referred to these regions as the first (on cation) and second (on anion) hydration layers hereafter. In the water density profiles on cations, we found a dip with the minimum at the distance of about 0.4 nm from the surface (where the distance is measured with respect to the plane going through the centers of the atoms in the outermost plane). The dips in the profiles on the cations correspond to the dark blob features above the first hydration layers (bright spots) on the cations in Figures 3a,b, which appear to be very similar to those observed experimentally.

Although it is often the case that the frequency shift map and water density map have many common features,[6,32] in principle, we cannot directly compare the frequency shift of the cantilever and the water density predicted by the MD simulations. Therefore, in this study, we obtained the interaction force profiles from the experimental and theoretical results to compare them directly. We use the STA model to convert the water density to the interaction force. In the original STA model, only the (number) density of the water oxygen atoms is taken into account. In this work, however, we use the molar density of the water (both oxygens and hydrogens) instead. In this way, the orientation of the water molecules is implicitly taken into account as some of the OH bonds do not lie parallel to the (001) plane (see Figure S2 in the Supporting Information). We noticed that using the molar density of water rather than the number density for oxygen alone greatly improves the force curves obtained from the STA model. Figure 4a,b shows the force versus distance curves on the KBr(001) and NaCl(001) surfaces calculated from the water density profiles presented in Figure 3b,d. We can find a large dip in the simulated force curves on the cations at the distance of about 0.3 nm, and a slightly smaller dip on the anions at the distance of about 0.4 nm, corresponding to the onset of the first

DOI: 10.1021/acs.jpcc.6b05651
J. Phys. Chem. C 2016, 120, 19714−19722

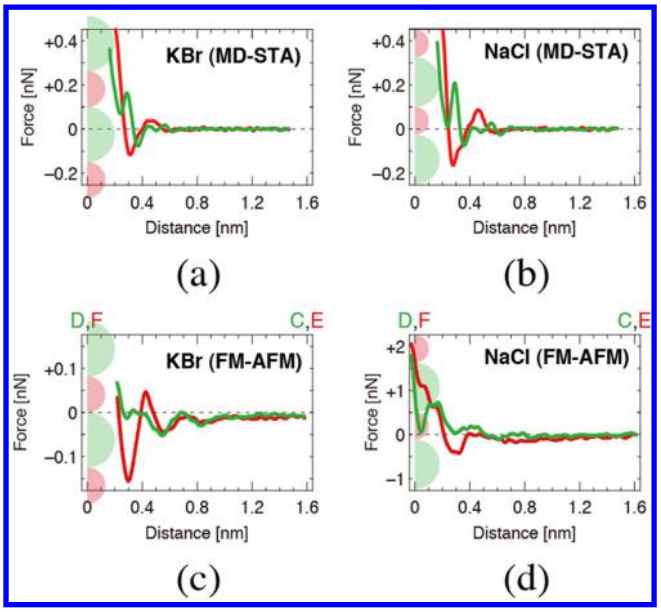

Figure 4. (a) Simulated force curves on the KBr(001) surface calculated by the STA model. Red and green curves represent those on K^+ and Br^- ions, respectively. (b) Simulated force curves on the NaCl(001) surface calculated by the STA model. Red and green curves represent those on Na^+ and Cl^- ions, respectively. (c) Experimental force curves on the KBr(001) surface converted from the frequency shift curves in Figure 2b. (d) Experimental force curves on the NaCl(001) surface converted from the frequency shift curves in Figure 2d.

(on cation) and second (on anion) hydration layers. The red and green semicircles in the figures represent the ionic radii of the ions. We also converted the experimental frequency shift curves in Figure 2b,d to the force curves; see Figure 4c,d. Because the tip oscillation amplitude was very small, general features observed in the frequency shift curves did not change from the frequency shift curves presented as Figure 2c,d. We assume that the characteristic dip we found in both the simulated and experimental force curves on the cations are the same, and we aligned the experimental force curves such that the dips in the force curves on the red curves are at 0.3 nm from the surface. By doing this, we found many features that are common in the simulated and experimental force curves. On the cations, the force curves exhibited a repulsive peak at the distance of 0.4 nm, and then an attractive dip at 0.3 nm, after which it monotonically increased. The green curves (over anions) show rather complicated features. They show a dip at about 0.25 nm in the simulated curves (green), whereas the experimental force curve on the NaCl(001) showed a dip at the 0.5 nm. We consider that the corresponding dip was not observed on the anion of the KBr(001) surface because the tip was not moved to such a close distance. The difference in the position of the dip on the Br^- ion for the simulated and experimental force curves is probably due to the relaxation of the tip in the experiment, which cannot be taken into account for the simulated curve (due to the assumptions in the STA model).

We sometimes observed the hydration layers by FM-AFM more pronounced than we expected from the MD simulation. The high sensitivity of the AFM to the hydration layers could be because of the presence of the solute ions as already mentioned. On the other hand, the physical tip structures that could cause the water confinement and the effect of the hydration structures on the tip have not been taken into account in the MD simulation. We need to perform explicit free energy calculation on the alkali halide crystals including the cluster tip model to understand the imaging mechanisms of the hydration layers by AFM, which is one of the ongoing projects.

It should be noted here that we also studied the (001) surfaces of NaF and LiF crystals. Although we often observed oscillatory hydration structures, we did not obtain 2D hydration structure contrasts as we observed for the KBr and NaCl surfaces (see Figures S3 and S4 in the Supporting Information). As it is likely the atomic-resolution images reflect the atomic periodicity within the hydration structures, we conclude that the low resolution in the NaF(001) and LiF(001) surfaces is partly because of the less distinct hydration layers on the ions, as predicted by the MD simulations (see Figure S5 and S6 in the Supporting Information). The MD simulations also showed that the orientation of the water molecules on the NaF(001) and LiF(001) surfaces are very much different from those on the KBr(001) and NaCl(001) surfaces (see Figure S2 and S7 in the Supporting Information). A relatively small ionic radius of the F^- ion, a small difference between the radii of anion and cation, and a small lattice constant can make the hydration structures very much different from those on the KBr(001) and NaCl(001) surfaces.

Step-Edge. We obtained a topographic image of a fluctuating step edge on the NaCl(001) surface as shown in Figure 5a. A stripe pattern with a spacing of 0.56 nm was observed, suggesting we achieved atomic resolution. In this image, the step line appears fuzzy, not straight, most likely because the atoms are attaching and detaching at the step edge.[33,34] Such fuzzy, or "frizzy", step edges have been observed in previous studies on the Ag(111) and Cu(001) surfaces in

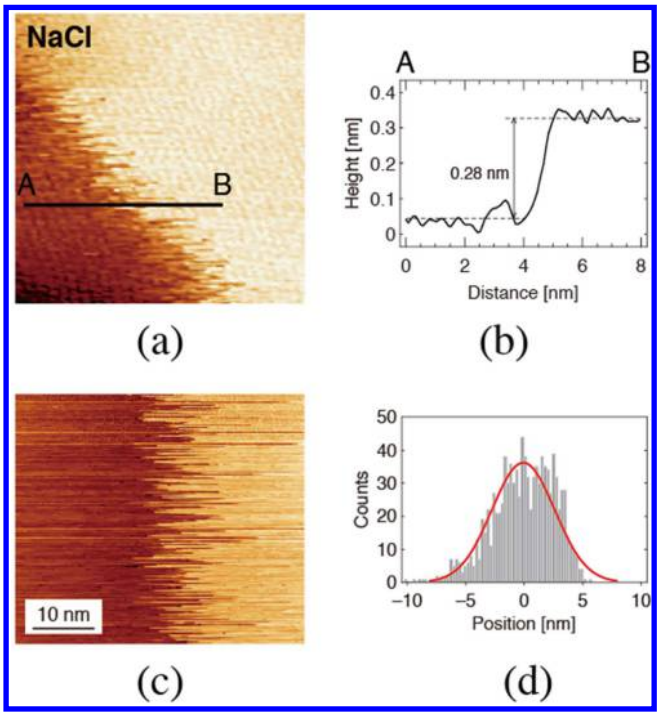

Figure 5. (a) Topographic image of NaCl(001) surface near a step edge. Scanned area was 13 nm × 13 nm. (b) Cross-sectional height profile measured along the line A–B indicated in (a). (c) Line-scan image of the step edge on the NaCl(001) surface. (d) Histogram of the step edge positions in 1000 scan lines.

DOI: 10.1021/acs.jpcc.6b05651
J. Phys. Chem. C 2016, 120, 19714–19722

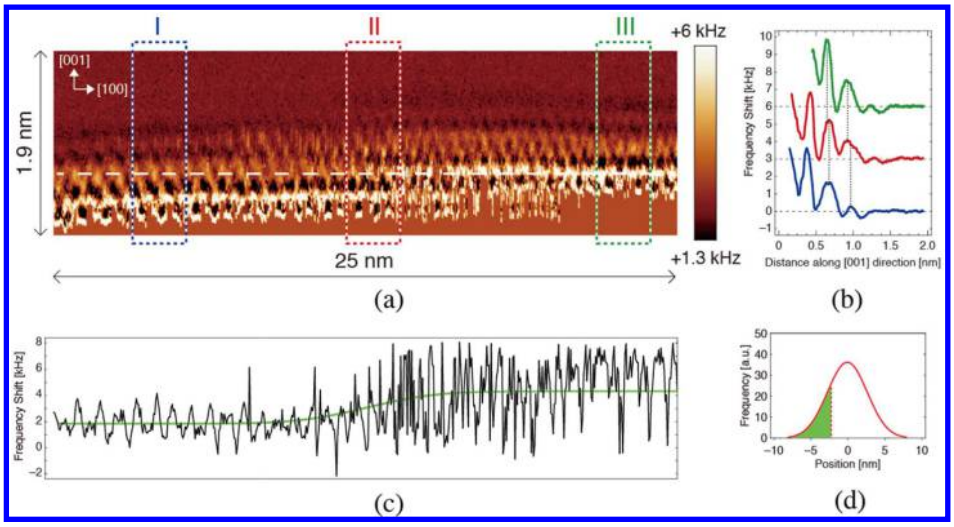

Figure 6. (a) 2D frequency shift image obtained along a scan line parallel to the [100] direction over a step edge on the NaCl(001) surface. Scanned area was 1.9 nm × 25 nm (A_{p-p} = 0.25 nm, Δf_{th} = 6 kHz). (d) Averaged frequency shift curves in the regions I, II, and III in (a). The curves for the regions II and III were shown with offsets of 3 kHz and 6 kHz, respectively. The vertical dotted lines in the figure illustrate that the two peaks in the region II curve can be decomposed to those in the region I and III curves. (c) Frequency shift profile measured on the dotted line indicated in (a). The green curve is a fitted curve profile to the frequency shift profile using a cumulative distribution function presented in (d).

vacuum[33,34] and the (010) surface of potassium dihydrophosphate (KDP) in liquid.[35] Because the scan frequency along the fast scan axis was about 5 Hz, the fuzzy appearance suggests that the step was moving with a time scale of shorter than 200 ms, and consequently, the kink site was moving on a much shorter time scale.[34] On the other hand, Figure 5b shows an example of the cross-sectional profile, which was measured along the line A−B indicated in Figure 5a. In this profile, a single height change of about 0.28 nm was observed within a width of about 0.5 nm along the [001] direction. If the step fluctuation were much faster than the scan, the cross-sectional profile would show multiple height changes during a single scan, which was not the case. Therefore, we consider that the step position was fluctuating with a time scale not much shorter than 100 ms.

In order to understand the fluctuations in more detail, we compared to our previous studies of dissolution of NaCl.[13,14] There, we used first-principles methods to show that the barrier for dissolution in water was of the order of 0.2−0.3 eV for both ions, clearly predicting a very rapid process on the time scale of FM-AFM simulations. We now further studied the association of the ions from solution back to the step-edge using the same methods to see if it would give some insight into the fluctuations seen experimentally. The obtained barriers were of the order of 0.1−0.2 eV, generally lower than the dissolution barriers and supporting the idea that the step-edge fluctuation can *exist* on the time scale of an FM-AFM measurement, in a state of repeated dissociation and association.

In an effort to measure the step roughness, we conducted a line-scan measurement across a step edge on the NaCl(001) surface. During the line-scan measurement, the tip was repeatedly scanned back and forth across the step edge on the same line at 10 Hz with the slow axis scan disabled. We collected 1000 cross-sectional profiles and analyzed the step edge position in each profile. Figure 5c shows a topographic image during the line scan measurement (the vertical direction representing time). Figure 5d shows a histogram of the step edge position in the scan profiles. The histogram shows a Gaussian distribution of the step edge position, which is consistent with the previous studies.[33,34] When defining the average position as zero, we found a standard deviation of approximately 2.6 nm.

Finally, we investigated the hydration structure near the step edge on the NaCl(001) surface. Figure 6a shows a 2D-Δf map measured across the same step edge shown in Figure 5c. The 2D frequency shift map was obtained by applying a triangular waveform of 10 Hz, and the number of recorded frequency shift versus distance curves was 512. Thus, the total acquisition time was the same as that for Figure 5c. We focus on three regions enclosed by the dotted rectangles in the figure, which are referred to as the regions I, II, and III hereafter. Regions I and III represent the area above the lower terrace and higher terrace, respectively. Because of the lateral and vertical drift of the relative tip position during the measurement, the tip did not exactly follow a single atomic row along the [100] direction. However, we obtained atomic-scale patterns along the [100] direction with a periodicity close to the unit cell (0.66 nm). The Δf contrast patterns in the regions I and III are very similar except for the displacement in the vertical direction. Figure 6b shows the averaged frequency shift curves in the regions I, II, and III. For clarity, the curves are shown with arbitrary offsets in the vertical direction. We note that the curves in the regions I and III are almost identical, expect for the displacement along the [001] direction. This indicates that the hydration structures on both the lower and upper terraces are the same, with the region II being slightly different. This is probably because the atoms are moving within the region II (due to dissolution and growth) with a time scale shorter than the time scale of the 2D frequency shift map measurement, which is about a minute. Because the curve in the region II is regarded as the time-average of those in the regions I and II, some peaks in the region II can be decomposed into two peaks. The vertical dotted lines in the figure illustrate that the two peaks in the region II curve can be decomposed to those in the region I and III curves. The topography image in this region is relatively jagged, especially at the right of region II, mainly because of the step motion. This can be understood as the frequency shift reaches the predetermined threshold Δf_{th} when the tip is

DOI: 10.1021/acs.jpcc.6b05651
J. Phys. Chem. C 2016, 120, 19714−19722

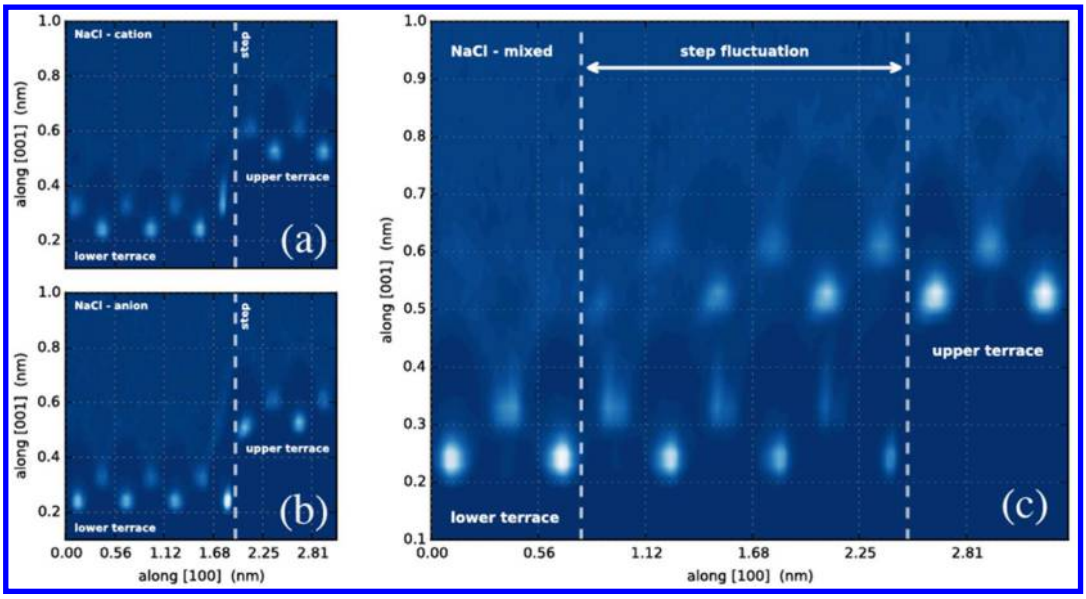

Figure 7. (a) 2D water density distribution along the [100] direction across a NaCl step edge terminated by a cation, (b) a similar 2D water density distribution, but this time for a step edge terminated by an anion. In (c) the time-averaged 2D water density distribution for a fluctuating step edge is shown.

brought very close to the surface, but in the region II this happens stochastically on either the higher or the lower terrace. Along the dashed white line in the [100] direction we measured the cross-sectional profile, see Figure 6a, with the corresponding frequency shift profile shown in Figure 6c. The magnitude of the quasiperiodic oscillation in the frequency shift is larger in region III because the tip is relatively closer to the surface. Especially in region II, the profile is noisier because of the step fluctuation. The profile can be fitted relatively well by a cumulative distribution function, $\Delta f(x) = c_1 + c_2\mathrm{Erf}(x/\sqrt{2}\sigma_f)$, with σ_f of 2.6 nm, as presented in Figure 6d, where c_1 and c_2 are the fitting parameters. During the 2D frequency shift mapping, the step moves around below the tip with a time scale of 100 ms or shorter, which is slower than the relaxation time of the hydration structures by several orders of magnitude. Therefore, it is reasonable that we can see the time-average of the hydration structures for the upper terrace and for the lower terrace.

To confirm that the imaging mechanisms of the region II in the 2D frequency shift map shown in Figure 6a was the time-average of the hydration structures at both the upper and lower terrace surrounding the step edge, we computed the hydration structures at the step edge from the MD simulations and then constructed the time-average of the 2D frequency shift map. Figure 7a,b shows the 2D density distributions of the water across the step edge, either with the upper terrace terminated with a cation (Figure 7a) or with an anion (Figure 7b). In order to construct a time-averaged density map, we overlaid several water densities (alternating the cation and anion terminated step densities) and shifted them with half the lattice constant along the [100] direction. This mimics the fact that when a cation dissolves from the step edge, the new step edge is terminated by an anion. Every density was weighted equally into the new time-averaged density, assuming that the system remains in the same edge-terminated situation a similar amount of time. Furthermore, this averaging approach assumes that whenever an ion dissolves from or adheres to the step the water density almost immediately adjusts to the new situation (which is a fair assumption as we noticed that already 10 ps of MD simulation time is sufficient to equilibrate a system). The result of this time-averaging on the computed water densities is shown in Figure 7c, demonstrating that this simple time-averaging method produces a water density very similar to the experimentally obtained cross-sectional 2D frequency shift map.

CONCLUSIONS

We showed subnanometer-scale hydration structures near step and terrace structures on the KBr(001) and NaCl(001) surfaces by 2D frequency shift mapping technique using FM-AFM. The hydration structures observed on the terraces agree well with predicted densities from MD simulations. We also measured the hydration structures at the step edge of the NaCl(001) surface. As the surface atoms were stochastically dissolving and absorbing, the location of the step edge was fluctuating, as predicted from our first-principles simulations. The hydration structure along the moving step edge was found to be the time-average of the hydration structure on both the upper terrace and those on the lower terrace. The time scale of the step motion was on the same order of the tip scan frequency, much longer than the time scale of the relaxation of water molecules by an order of magnitude. Despite this large difference in time scales, this combination of experimental and theoretical methods is generally applicable to study local hydration structures that dynamically change at the surfaces of soluble crystals, particularly if one considers the recent advances in high speed FM-AFM.[36]

ASSOCIATED CONTENT

Supporting Information

The Supporting Information is available free of charge on the ACS Publications website at DOI: 10.1021/acs.jpcc.6b05651.

Additional experimental data on the NaCl(001), NaF(001), and LiF(001) surfaces. 2D correlation map of the angles of either OH bond of the water molecules. 2D water density distributions and 1D water density

DOI: 10.1021/acs.jpcc.6b05651
J. Phys. Chem. C 2016, 120, 19714−19722

profiles on the NaF(001) and LiF(001) surfaces by MD simulations. (PDF)

AUTHOR INFORMATION

Corresponding Authors

*E-mail: keicoba@iic.kyoto-u.ac.jp. Tel: +81-75-383-2307.
*E-mail: adam.foster@aalto.fi. Tel.: +358-50-4333097.

Notes

The authors declare no competing financial interest.

ACKNOWLEDGMENTS

This work was supported by Grants-in-Aid for Scientific Research from Japan Society for the Promotion of Science, the Academy of Finland through its Centres of Excellence Program (project no. 915804), EU project PAMS (contract no. 610446), and acknowledge use of the CSC, Helsinki for computational resources.

REFERENCES

(1) Cheng, L.; Fenter, P.; Nagy, K. L.; Schlegel, M. L.; Sturchio, N. C. Molecular-Scale Density Oscillations in Water Adjacent to a Mica Surface. *Phys. Rev. Lett.* **2001**, *87*, 156103.

(2) Bennema, P. Interpretation of the Relation between the Rate of Crystal Growth from Solution and the Relative Supersaturation at Low Supersaturation. *J. Cryst. Growth* **1967**, *1*, 287−292.

(3) Kimura, K.; Ido, S.; Oyabu, N.; Kobayashi, K.; Hirata, Y.; Imai, T.; Yamada, H. Visualizing Water Molecule Distribution by Atomic Force Microscopy. *J. Chem. Phys.* **2010**, *132*, 194705.

(4) Fukuma, T.; Ueda, Y.; Yoshioka, S.; Asakawa, H. Atomic-Scale Distribution of Water Molecules at the Mica-Water Interface Visualized by Three-Dimensional Scanning Force Microscopy. *Phys. Rev. Lett.* **2010**, *104*, 016101.

(5) Hiasa, T.; Kimura, K.; Onishi, H.; Ohta, M.; Watanabe, K.; Kokawa, R.; Oyabu, N.; Kobayashi, K.; Yamada, H. Aqueous Solution Structure over α-Al_2O_3(01−12) Probed by Frequency-Modulation Atomic Force Microscopy. *J. Phys. Chem. C* **2010**, *114*, 21423−21426.

(6) Kobayashi, K.; Oyabu, N.; Kimura, K.; Ido, S.; Suzuki, K.; Imai, T.; Tagami, K.; Tsukada, M.; Yamada, H. Visualization of Hydration Layers on Muscovite Mica in Aqueous Solution by Frequency-Modulation Atomic Force Microscopy. *J. Chem. Phys.* **2013**, *138*, 184704.

(7) Labuda, A.; Kobayashi, K.; Kiracofe, D.; Suzuki, K.; Grütter, P. H.; Yamada, H. Comparison of Photothermal and Piezoacoustic Excitation Methods for Frequency and Phase Modulation Atomic Force Microscopy in Liquid Environments. *AIP Adv.* **2011**, *1*, 022136.

(8) Kobayashi, N.; Itakura, S.; Asakawa, H.; Fukuma, T. Atomic-Scale Processes at the Fluorite−Water Interface Visualized by Frequency Modulation Atomic Force Microscopy. *J. Phys. Chem. C* **2013**, *117*, 24388−24396.

(9) Araki, Y.; Tsukamoto, K.; Takagi, R.; Miyashita, T.; Oyabu, N.; Kobayashi, K.; Yamada, H. Direct Observation of the Influence of Additives on Calcite Hydration by Frequency Modulation Atomic Force Microscopy. *Cryst. Growth Des.* **2014**, *14*, 6254−6260.

(10) *CRC Handbook of Chemistry and Physics*, 96th ed.; Haynes, W. M., Ed.; CRC Press: Boca Raton, FL, 2015.

(11) Engkvist, O.; Stone, A. J. Adsorption of Water on NaCl(001). I. Intermolecular Potentials and Low Temperature Structures. *J. Chem. Phys.* **1999**, *110*, 12089−12096.

(12) Engkvist, O.; Stone, A. J. Adsorption of Water on the NaCl(001) Surface. III. Monte Carlo Simulations at Ambient Temperatures. *J. Chem. Phys.* **2000**, *112*, 6827−6833.

(13) Holmberg, N.; Chen, J.-S.; Foster, A. S.; Laasonen, K. Dissolution of NaCl Nanocrystals: an *ab initio* Molecular Dynamics Study. *Phys. Chem. Chem. Phys.* **2014**, *16*, 17437−17446.

(14) Chen, J.-C.; Reischl, B.; Spijker, P.; Holmberg, N.; Laasonen, K.; Foster, A. S. *Ab initio* Kinetic Monte Carlo Simulations of Dissolution at the NaCl−Water Interface. *Phys. Chem. Chem. Phys.* **2014**, *16*, 22545−22554.

(15) Nagashima, K.; Abe, M.; Morita, S.; Oyabu, N.; Kobayashi, K.; Yamada, H.; Ohta, M.; Kokawa, R.; Murai, R.; Matsumura, H.; et al. Molecular Resolution Investigation of Tetragonal Lysozyme (110) Face in Liquid by Frequency-Modulation Atomic Force Microscopy. *J. Vac. Sci. Technol. B* **2010**, *28*, C4C11−C4C14.

(16) Kobayashi, K.; Yamada, H.; Itoh, H.; Horiuchi, T.; Matsushige, K. Analog Frequency Modulation Detector for Dynamic Force Microscopy. *Rev. Sci. Instrum.* **2001**, *72*, 4383−4387.

(17) Kobayashi, K.; Yamada, H.; Matsushige, K. Reduction of Frequency Noise and Frequency Shift by Phase Shifting Elements in Frequency Modulation Atomic Force Microscopy. *Rev. Sci. Instrum.* **2011**, *82*, 033702.

(18) Sader, J. E.; Jarvis, S. P. Accurate Formulas for Interaction Force and Energy in Frequency Modulation Force Spectroscopy. *Appl. Phys. Lett.* **2004**, *84*, 1801−1803.

(19) Brooks, B. R.; Brooks, C. L., III; MacKerell, A. D., Jr.; Nilsson, L.; Petrella, R. J.; Roux, B.; Won, Y.; Archontis, G.; Bartels, C.; Boresch, S.; et al. CHARMM: the Biomolecular Simulation Program. *J. Comput. Chem.* **2009**, *30*, 1545−1614.

(20) Phillips, J. C.; Braun, R.; Wang, W.; Gumbart, J.; Tajkhorshid, E.; Villa, E.; Chipot, C.; Skeel, R. D.; Kalé, L.; Schulten, K. Scalable Molecular Dynamics with NAMD. *J. Comput. Chem.* **2005**, *26*, 1781−1802.

(21) Humphrey, W.; Dalke, A.; Schulten, K. VMD: Visual Molecular Dynamics. *J. Mol. Graphics* **1996**, *14*, 33−38.

(22) Michaud-Agrawal, N.; Denning, E. J.; Woolf, T. B.; Beckstein, O. MDAnalysis: A Toolkit for the Analysis of Molecular Dynamics Simulations. *J. Comput. Chem.* **2011**, *32*, 2319−2327.

(23) Ricci, M.; Spijker, P.; Stellacci, F.; Molinari, J.-F.; Voitchovsky, K. Direct Visualization of Single Ions in the Stern Layer of Calcite. *Langmuir* **2013**, *29*, 2207−2216.

(24) Ricci, M.; Spijker, P.; Voitchovsky, K. Water-Induced Correlation between Single Ions Imaged at the Solid-Liquid Interface. *Nat. Commun.* **2014**, *5*, 4400.

(25) Fukuma, T.; Reischl, B.; Kobayashi, N.; Spijker, P.; Canova, F. F.; Miyazawa, K.; Foster, A. S. Mechanism of Atomic Force Microscopy Imaging of Three-Dimensional Hydration Structures at a Solid-Liquid Interface. *Phys. Rev. B: Condens. Matter Mater. Phys.* **2015**, *92*, 155412.

(26) Reischl, B.; Watkins, M.; Foster, A. S. Free Energy Approaches for Modeling Atomic Force Microscopy in Liquids. *J. Chem. Theory Comput.* **2013**, *9*, 600−608.

(27) Watkins, M.; Reischl, B. A Simple Approximation for Forces Exerted on an AFM Tip in Liquid. *J. Chem. Phys.* **2013**, *138*, 154703.

(28) Amano, K.; Suzuki, K.; Fukuma, T.; Takahashi, O.; Onishi, H. The Relationship between Local Liquid Density and Force Applied on a Tip of Atomic Force Microscope: A Theoretical Analysis for Simple Liquids. *J. Chem. Phys.* **2013**, *139*, 224710−7.

(29) Miyazawa, K.; Kobayashi, N.; Watkins, M.; Shluger, A. L.; Amano, K.; Fukuma, T. *Nanoscale* **2016**, *8*, 7334−7342.

(30) Du, H.; Miller, J. D. Interfacial Water Structure and Surface Charge of Selected Alkali Chloride Salt Crystals in Saturated Solutions: A Molecular Dynamics Modeling Study. *J. Phys. Chem. C* **2007**, *111*, 10013−10022.

(31) Joung, I. S.; Cheatham, T. E., III Molecular Dynamics Simulations of the Dynamic and Energetic Properties of Alkali and Halide Ions Using Water-Model-Specific Ion Parameters. *J. Phys. Chem. B* **2009**, *113*, 13279−13290.

(32) Spijker, P.; Hiasa, T.; Musso, T.; Nishioka, R.; Onishi, H.; Foster, A. S. Understanding the Interface of Liquids with an Organic Crystal Surface from Atomistic Simulations and AFM Experiments. *J. Phys. Chem. C* **2014**, *118*, 2058−2066.

(33) Wolf, J. F.; Vicenzi, B.; Ibach, H. Step Roughness on Vicinal Ag(111). *Surf. Sci.* **1991**, *249*, 233−236.

(34) Poensgen, M.; Wolf, J. F.; Frohn, J.; Giesen, M.; Ibach, H. Step dynamics on Ag(111) and Cu(100) surfaces. *Surf. Sci.* **1992**, *274*, 430−440.

DOI: 10.1021/acs.jpcc.6b05651
J. Phys. Chem. C 2016, 120, 19714−19722

(35) De Yoreo, J. J.; Zepeda-Ruiz, L. A.; Friddle, R. W.; Qiu, S. R.; Wasylenki, L. E.; Chernov, A. A.; Gilmer, G. H.; Dove, P. M. Rethinking Classical Crystal Growth Models through Molecular Scale Insights: Consequences of Kink-Limited Kinetics. *Cryst. Growth Des.* **2009**, *9*, 5135−5144.
(36) Miyata, K.; Miyazawa, K.; Akrami, S. M. R.; Fukuma, T. Improvements in Fundamental Performance of Liquid-Environment Atomic Force Microscopy with True Atomic Resolution. *Jpn. J. Appl. Phys.* **2015**, *54*, 08LA03.

DOI: 10.1021/acs.jpcc.6b05651
J. Phys. Chem. C 2016, 120, 19714−19722